# Chapter 9
# Extraction of Boundary Impedance via Traveling Wave Analysis

**William C. Rogers, Mohammad I. Albakri, and Pablo A. Tarazaga**

**Abstract** Boundary conditions present in realistic environments are not often well represented by classical dynamic models. Extraction of accurate boundary conditions is necessary for substructuring applications and for meaningful environmental tests. The work herein addresses this problem via a novel method of boundary condition extraction utilizing traveling waves. Although it is possible to produce steady-state progressive waves in finite media, the excitation conditions required to do so are highly sensitive to the impedance of the boundary conditions. This study investigates the potential of leveraging this sensitivity to extract boundary conditions of a structure or a subsection of a larger structure. Traveling waves are generated using a modified two-point excitation, while boundary conditions are extracted by identifying excitation conditions corresponding to pure traveling waves. An example case is shown for an Euler-Bernoulli beam, where the boundary impedances are extracted with high accuracy.

**Keywords** Traveling waves · Impedance · Dynamic modeling

## Introduction

Structure-bone traveling waves have been the subject of study for decades. All vibrating media experience wave propagation. The most common vibration behavior is standing waves, which is a steady-state phenomenon. These are often present in finite structures seen in modal analysis [1], these are the result of superimposed traveling waves in the structure. Generating propagating waves in finite media has been investigated in many studies, such as driving wave-driven motors [2, 3, 4], propelling particulates for high-precision pumps [5, 6], and replicating the behavior of the cochlear membrane in the human ear [7]. Of particular interest to this study is the influence of the boundary conditions on the wave propagation behavior of a finite structure. It has been noted by several authors that for finite media, ideal excitation conditions to generate dominantly traveling waves are sensitive to the boundary conditions of the structure [8, 9, 10]. This work is the first to demonstrate that this sensitivity allows for the extraction of the boundary impedance.

A pure traveling wave is one that propagates along a structure without reflection. There are three well-known methods of producing traveling waves in finite media with two exciters: active sink [11], impedance matching [12], and two-point (or two-mode) excitation [13]. Although only one of these methods includes the term "impedance," all three can be described by exciting a wave at one point in the structure and matching the impedance at a later point, where the wave is absorbed.

William C. Rogers · Pablo A. Tarazaga
Fusion of Analysis, Simulation, and Testing (FAST) Lab, Texas A&M University, College Station, TX 77840, United States of America
e-mail: wcrogers42@tamu.edu; ptarazaga@tamu.edu

William C. Rogers · Mohammad I. Albakri
Smart Materials and Structures Research Lab College of Science and Engineering, Hamad Bin Khalifa University, Education City, Doha, Qatar
e-mail: wcrogers42@tamu.edu; malbakri@hbku.edu.qa

Mohammad I. Albakri
Texas A&M University at Qatar, Education City, Doha, Qatar
e-mail: malbakri@hbku.edu.qa



Kristin B. Zimmerman, PhD (eds.), *Topics in Modal Analysis & Parameter Identification in Structural Dynamics, 2026, Vol. 8*, Conference Proceedings of the Society for Experimental Mechanics Series, https://doi.org/10.1007/978-8-743-81447-4_9

This is effectively achieved by exciting the structure at two points with a common frequency and a complex amplitude ratio between the two points. Both active sink and impedance matching allow these complex ratios to have different magnitudes. In contrast, two-point excitation forces have equal magnitude excitation with only a phase offset between the excitation points.

It was noted by Gabai and Bucher that the active sink method is susceptible to the boundary conditions of the structure [9]. In the original work presenting the active sink method, an Euler-Bernoulli beam was modeled as a waveform transforming along a waveguide. The excitation conditions necessary to produce a pure traveling wave were extracted from the formulation, but this requires an accurate model of the boundaries [11]. Later work by Gabai and Bucher [9] has shown that for cases of a single waveguide, this formulation can be written treating the forces as boundary elements and rearranging the characteristic equation to solve exactly for the complex forcing ratio. As noted in [9], even for this simplified case, the purity of the traveling waves generated by this predicted complex ratio is sensitive to the boundary conditions that must be known *a priori* for an exact calculation. Often, this shortcoming is accounted for with manual tuning of the complex ratio to achieve pure traveling waves.

This sensitivity of traveling waves to boundary conditions begs the question sought to be answered in this paper. Can the boundary conditions be extracted via the excitation conditions necessary for the generation of traveling waves? Understanding the boundary impedances of a structure is of particular interest for researchers in the area of vibration qualification testing [14], allowing for the design of better test apparatuses for environmental vibration testing. This approach is also convenient in that it does not require equally spaced measurement points and can extract properties using relatively low-magnitude excitation. These methods are scalable to higher dimensions and are agnostic to the direction of displacement included in the formulation.

## Methodology

This section deals with the theoretical basis of the work. First, an analytical formulation for generating a pure traveling wave for an Euler-Bernoulli beam under fully generalized boundary conditions is presented. Next, the method for extracting boundary impedances based on the loading conditions required for pure traveling waves will be presented. Finally, a discussion is included on how the necessary information for this method is extracted in a realistic experimental environment.

### *Extraction of Boundary Impedances via Generation of Traveling Waves*

To approximate a beam with generalized boundary conditions, consider a beam with springs and dampers acting linearly and torsionally in addition to masses acting on both sides of the beam (see Figure 1). The solution of the beam is assumed to be separable and of the form [15],

$$w(x,t) = W(x)e^{j\omega t} = \left[C_1 e^{-j\beta x} + C_2 e^{j\beta x} + C_3 e^{-\beta x} + C_4 e^{\beta x}\right] e^{j\omega t}. \tag{1}$$

For the case where forces are applied at the beam's ends, the boundary conditions for an Euler-Bernoulli beam of length $L$ under these conditions are then [15],

$$\begin{aligned} EIw_{,xxx}(0,t) + k_1 w(0,t) + c_1 \dot{w}(0,t) + m_1 \ddot{w}(0,t) &= F_1 e^{j\omega t}, \\ -EIw_{,xxx}(L,t) + k_2 w(L,t) + c_2 \dot{w}(L,t) + m_2 \ddot{w}(L,t) &= F_2 e^{j\omega t}, \\ -EIw_{,xx}(0,t) + k_{t1} w_{,x}(0,t) + c_{t1} \dot{w}_{,x}(0,t) &= M_1 e^{j\omega t}, \\ EIw_{,xx}(L,t) + k_{t2} w_{,x}(L,t) + c_{t2} \dot{w}_{,x}(L,t) &= M_2 e^{j\omega t}. \end{aligned} \tag{2}$$

(3)

These boundaries can be rearranged into a system of equations,

$$\boldsymbol{A}\boldsymbol{c} = \boldsymbol{F}, \tag{4}$$

where $\boldsymbol{c} = \{C_1\ C_2\ C_3\ C_4\}^{\mathrm{T}}$ , $\boldsymbol{F} = \{F_1\ F_2\ M_1\ M_2\}^{\mathrm{T}}$, and $\boldsymbol{A}$ is a $4 \times 4$ matrix. The steady-state solution then for the system can then be solved by inverting the $\boldsymbol{A}$ matrix to solve for the $C_i$ terms. The terms of the $\boldsymbol{A}$ matrix can be written as,

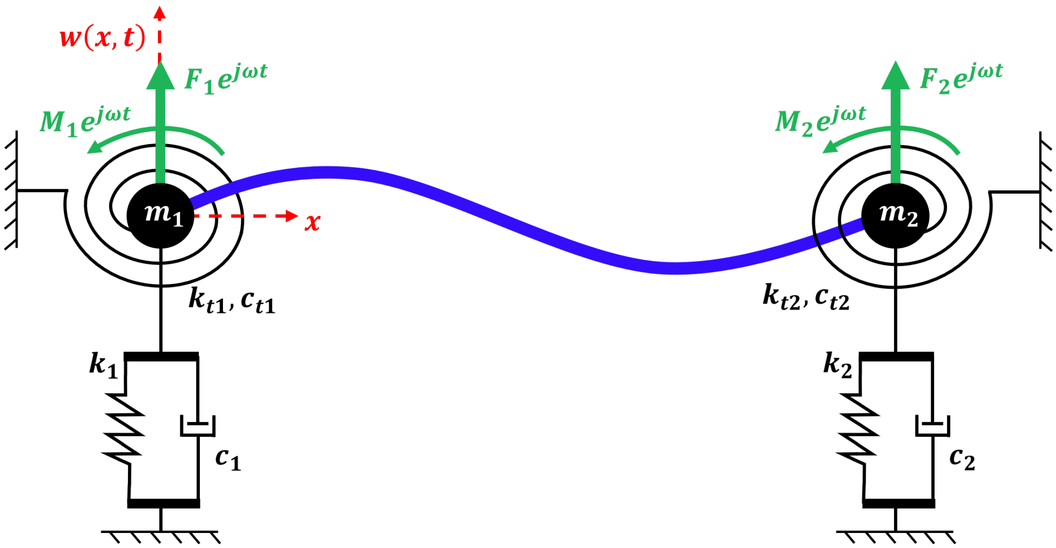


**Fig. 1** Beam with generalized boundary conditions and applied loads

$$\begin{aligned}
A_{11} &= j\omega Z_1 + j\omega Z_V, & A_{12} &= j\omega Z_1 - j\omega Z_V,\\
A_{13} &= j\omega Z_1 - \omega Z_V, & A_{14} &= j\omega Z_1 + \omega Z_V,\\
A_{21} &= (j\omega Z_2 - j\omega Z_V)e^{-j\beta L}, & A_{22} &= (j\omega Z_2 + j\omega Z_V)e^{j\beta L},\\
A_{23} &= (j\omega Z_2 + \omega Z_V)e^{-\beta L}, & A_{24} &= (j\omega Z_2 - \omega Z_V)e^{\beta L},\\
A_{31} &= \omega Z_{t1} - \omega Z_M, & A_{32} &= -\omega Z_{t1} - \omega Z_M,\\
A_{33} &= -j\omega Z_{t1} + \omega Z_M, & A_{34} &= j\omega Z_{t1} + \omega Z_M,\\
A_{41} &= (\omega Z_{t2} + \omega Z_M)e^{-j\beta L}, & A_{42} &= (-\omega Z_{t2} + \omega Z_M)e^{j\beta L},\\
A_{43} &= (-j\omega Z_{t2} - \omega Z_M)e^{-\beta L}, & A_{44} &= (j\omega Z_{t2} - \omega Z_M)e^{\beta L},
\end{aligned} \tag{5}$$

where the impedances of the boundaries are defined as $Z_i = c_i + jm_i(\omega^2 - \omega_i^2)/\omega$, $Z_{ti} = \beta(c_{ti} - jk_{ti}/\omega)$, and $\omega_i^2 = k_i/m_i$ and the impedances of the beam are $Z_V = EI\beta^3/\omega$ and $Z_M = -EI\beta^2/\omega$ for shear forces and moments respectively (where $i = 1, 2$). For this study, it is assumed that the properties and vibration behavior of the beam $(Z_V, Z_M)$ are known. This is comparable to a case where a test specimen can be removed from its environment and tested independently.

The loading vector terms can be arranged to define the loading ratios

$$\begin{aligned}
Q_F &\equiv \frac{F_1}{F_2}, & Q_{11} &\equiv \frac{F_1}{M_1}, & Q_{12} &\equiv \frac{F_1}{M_2},\\
Q_M &\equiv \frac{M_1}{M_2}, & Q_{22} &\equiv \frac{F_2}{M_2}, & Q_{21} &\equiv \frac{F_2}{M_1}.
\end{aligned} \tag{6}$$

These ratios are then analogous to the complex loading ratios for the active sink method [11]. Although only three of these terms are necessary to define the excitation conditions required for a pure traveling wave (since only three are independent), all six have been defined explicitly above for convenience. For the case of the pure right-moving traveling wave, it is known that $C_2 = C_3 = C_4 = 0$ and $C_1 \neq 0$. Given this, we can relate our loading ratios in Equation 6 to the terms in the first column of $\boldsymbol{A}$. These relations are then

$$\begin{aligned}
Q_F^R &= \frac{A_{11}}{A_{21}}, & Q_{11}^R &= \frac{A_{11}}{A_{31}}, & Q_{12}^R &= \frac{A_{11}}{A_{41}},\\
Q_M^R &= \frac{A_{31}}{A_{41}}, & Q_{22}^R &= \frac{A_{21}}{A_{41}}, & Q_{21}^R &= \frac{A_{21}}{A_{31}}.
\end{aligned} \tag{7}$$

Each of these ratios in Equation 7 can be used to define an expression relating two of the boundary impedance terms to the impedance terms of the beam. Substituting the full expressions from the Equations in 5 into Equation 7 and rearranging the six equations into a new matrix yields the form,

$$\boldsymbol{\Gamma}_R \boldsymbol{Z}_{BC} = \boldsymbol{\Omega}_R. \tag{8}$$

The terms of Equation 8 are expanded as,

$$\boldsymbol{Z}_{BC} = \{Z_1 \quad Z_2 \quad Z_{t1} \quad Z_{t2}\}^{\mathrm{T}}, \tag{9}$$

$$\boldsymbol{\Gamma}_R = \begin{bmatrix} 1 & -Q_F^R e^{-j\beta L} & 0 & 0 \\ 0 & 0 & 1 & -Q_M^R e^{-j\beta L} \\ -j & 0 & Q_{11}^R & 0 \\ 0 & j & 0 & -Q_{22}^R \\ 0 & j & -Q_{21}^R e^{j\beta L} & 0 \\ j & 0 & 0 & -Q_{12}^R e^{j\beta L} \end{bmatrix}, \tag{10}$$

$$\boldsymbol{\Omega}_R = Z_V \begin{Bmatrix} -(1+Q_F^R e^{-j\beta L}) \\ 0 \\ j \\ j \\ j \\ -j \end{Bmatrix} + Z_M \begin{Bmatrix} 0 \\ (1+Q_M^R e^{-j\beta L}) \\ Q_{11}^R \\ Q_{22}^R \\ -Q_{21}^R e^{j\beta L} \\ Q_{12}^R e^{-j\beta L} \end{Bmatrix}, \tag{11}$$

where the superscript $(\cdot)^R$ and subscript $(\cdot)_R$ have been included to indicate that these ratios and matrices are defined in terms of a pure right traveling wave case. This matrix equation is overdefined, so an exact solution is not possible. An approximate solution is possible by calculating the pseudoinverse of the $\boldsymbol{\Gamma}_R$; however, the rank of $\boldsymbol{\Gamma}_R$ is 3, thus the pseudoinverse is ill-conditioned. The loading ratios in Equation 6 can also be related to a pure left-moving traveling wave case (where $C_1 = C_3 = C_4 = 0$ and $C_2 \neq 0$). Applying this condition, the ratios in Equation 6 are expressed as,

$$\begin{aligned} Q_F^L &= \frac{A_{12}}{A_{22}}, \quad Q_{11}^L = \frac{A_{12}}{A_{32}}, \quad Q_{12}^L = \frac{A_{12}}{A_{42}}, \\ Q_M^L &= \frac{A_{32}}{A_{42}}, \quad Q_{22}^L = \frac{A_{22}}{A_{42}}, \quad Q_{21}^L = \frac{A_{22}}{A_{32}}. \end{aligned} \tag{12}$$

The six ratios can again be rearranged into a matrix form,

$$\boldsymbol{\Gamma}_L \boldsymbol{Z}_{BC} = \boldsymbol{\Omega}_L, \tag{13}$$

where these terms are expanded

$$\boldsymbol{\Gamma}_L = \begin{bmatrix} -1 & -Q_F^L e^{j\beta L} & 0 & 0 \\ 0 & 0 & -1 & Q_M^L e^{j\beta L} \\ j & 0 & Q_{11}^L & 0 \\ 0 & j & 0 & Q_{22}^L \\ 0 & je^{j\beta L} & Q_{21}^L & 0 \\ j & 0 & 0 & -Q_{12}^L e^{j\beta L} \end{bmatrix}, \tag{14}$$

$$\boldsymbol{\Omega}_L = Z_V \begin{Bmatrix} -(1+Q_F^L e^{j\beta L}) \\ 0 \\ j \\ -j \\ -je^{j\beta L} \\ j \end{Bmatrix} + Z_M \begin{Bmatrix} 0 \\ (1+Q_M^L e^{j\beta L}) \\ -Q_{11}^L \\ Q_{22}^L \\ -Q_{21}^L \\ Q_{12}^L e^{-\beta L} \end{Bmatrix}, \tag{15}$$

where the superscript $(\cdot)^L$ and subscript $(\cdot)_L$ are introduced to indicate that these conditions are associated with the left-moving traveling wave. Equation 13 is similar to Equation 8 in that $\boldsymbol{\Gamma}_L$ is also rank 3, resulting in an ill-conditioned pseudoinverse. Although equations 8 and 13 alone are insufficient to extract the impedances accurately, these can be combined with far better success. The equations both relate the same boundary impedance vector $\boldsymbol{Z}_{BC}$, so the equations can be appended as

$$\boldsymbol{\Gamma}_{RL} \boldsymbol{Z}_{BC} = \begin{bmatrix} \boldsymbol{\Gamma}_R \\ \boldsymbol{\Gamma}_L \end{bmatrix} \boldsymbol{Z}_{BC} = \begin{Bmatrix} \boldsymbol{\Omega}_R \\ \boldsymbol{\Omega}_L \end{Bmatrix}. \tag{16}$$

By appending the $\boldsymbol{\Gamma}_R$ and $\boldsymbol{\Gamma}_L$ the resulting matrix, $\boldsymbol{\Gamma}_{RL}$, has a rank of 4 and a well-conditioned pseudoinverse. Thus, the impedance of the boundaries can be approximated from the loading ratios associated with pure traveling waves. The accuracy of this approximation will be evaluated for an example case in the Results section.

## Results

This section will consider a case study where complex boundary impedances are extracted from a known Euler-Bernoulli beam. The beam under consideration in this study has dimensions 10 mm $\times$ 1 mm $\times$ 1 m, a Young's Modulus of 70 GPa, and a density of 2700 kg/m$^3$. The boundary impedances are calculated according to the boundary terms in Table 1. To extract the boundary impedances, the excitation conditions are identified for a pure right and left traveling wave for each frequency. Examples for a low and a high frequency case are shown in Figures 2 and 3. These waveforms have been generated using the associated forcing ratios that have been defined in Equations 7 and 12. For the benefit of the reader, the ideal loading ratios for these traveling wave examples are included in Table 2. These ratios are complex, so they have been reported in terms of their magnitude and their phase in degrees. These waveform examples are both calculated for $F_2 = 1$ kN, defining the other three loading terms using the calculated ratios in Table 2. The traveling waves have been plotted using a spatial resolution of 500 points to ensure no spatial aliasing and were sampled for 50 points temporally across one period $T$. The time axes have been normalized by their respective periods to improve readability.

**Table 1** Boundary condition terms used for this case study

| Intertial | Elastic | Dissapitive |
|---|---|---|
| $m_1 = 50$ g | $k_1 = 300$ N/m | $c_1 = 30$ N·s/m |
| $m_2 = 20$ g | $k_2 = 100$ N/m | $c_2 = 20$ N·s/m |
| | $k_{t1} = 70$ N·m/m | $c_{t1} = 5$ N·m·s/m |
| | $k_{t2} = 30$ N·m/m | $c_{t2} = 4$ N·m·s/m |

**Table 2** Loading ratios producing the pure traveling waves for frequencies 20 Hz and 2.5 kHz

| | $\lvert Q_F^R \rvert$ | $\lvert Q_{11}^R \rvert$ | $\lvert Q_{12}^R \rvert$ | $\lvert Q_F^L \rvert$ | $\lvert Q_{11}^L \rvert$ | $\lvert Q_{12}^L \rvert$ |
|---|---|---|---|---|---|---|
| 20 Hz | 1.55 | 0.60 | 0.83 | 1.46 | 0.64 | 0.81 |
| 2.5 kHz | 2.50 | 1.52 | 1.90 | 2.49 | 1.52 | 1.90 |
| | $\angle Q_F^R$ | $\angle Q_{11}^R$ | $\angle Q_{12}^R$ | $\angle Q_F^L$ | $\angle Q_{11}^L$ | $\angle Q_{12}^L$ |
| 20 Hz | $172°$ | $103°$ | $-89.5°$ | $-167°$ | $-76°$ | $111°$ |
| 2.5 kHz | $163°$ | $177°$ | $-19.4°$ | $-160°$ | $-1.84°$ | $-165°$ |

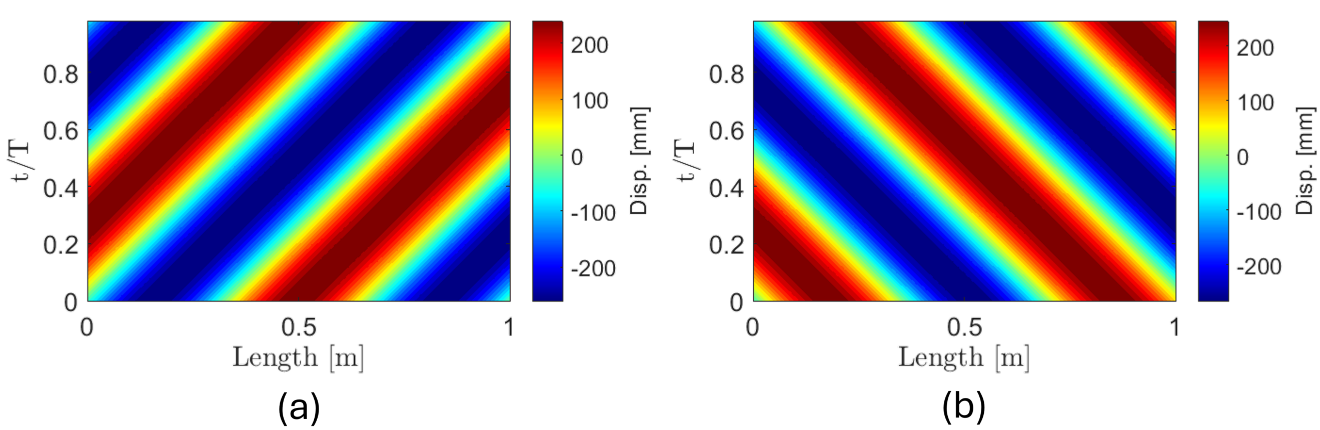


**Fig. 2** Contour of a propagating wave for the pure (a) right-moving and (b) left-moving traveling waves associated with $\omega = 20$ Hz

It was mentioned in the Methodolgy that of the cases presented, only Equation 16 yields a well-conditioned pseudoinverse; thus, for brevity, only the results of this approximation are reported. The loading ratios to produce pure left and right traveling waves are calculated for a frequency range of $\omega \in (0, 5)$ kHz at 12 evenly distributed frequency lines. For each frequency, the loading ratios are plugged into Equation 16 and the boundary impedances are extracted and are plotted against the exact values in Figures 4 and 5. The average error across all four of the boundary impedances is on the order of $10^{-15}$,

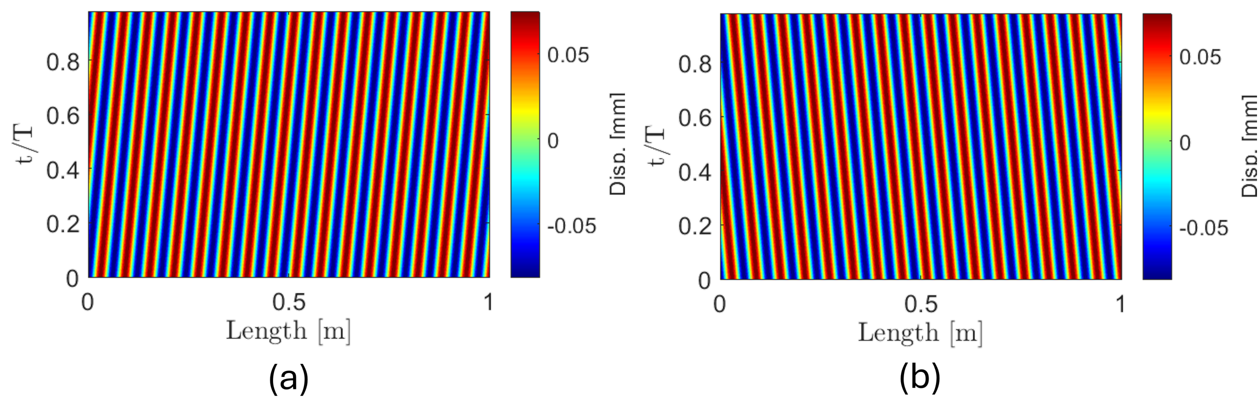


**Fig. 3** Contour of a propagating wave for the pure (a) right-moving and (b) left-moving traveling waves associated with $\omega = 2.5$ kHz

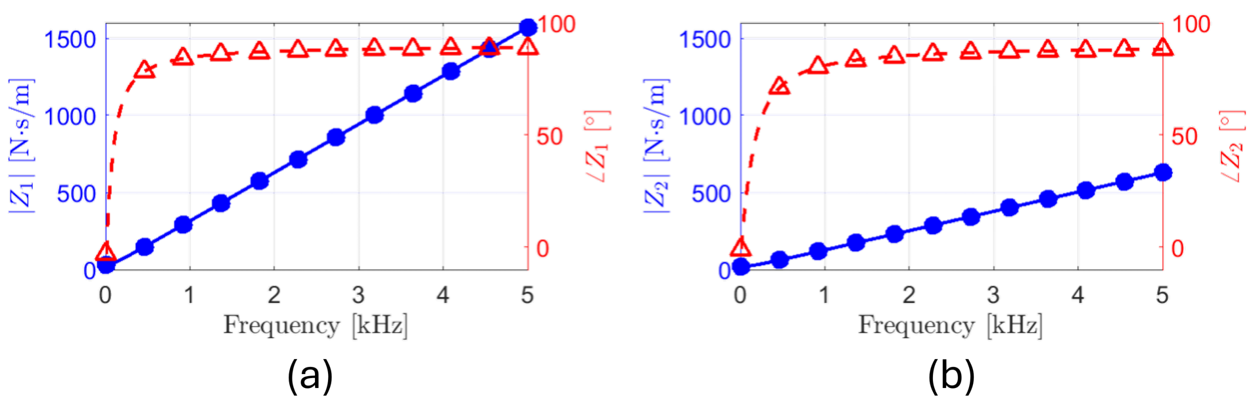


**Fig. 4** Magnitude (blue) and phase (red) of the exact and approximated transverse impedances ($Z_1$, $Z_2$). Exact impedances for the (a) left and (b) right-hand sides of the beam are in solid blue and dashed red lines, while the approximated values are dotted for the magnitude and triangles for the phase

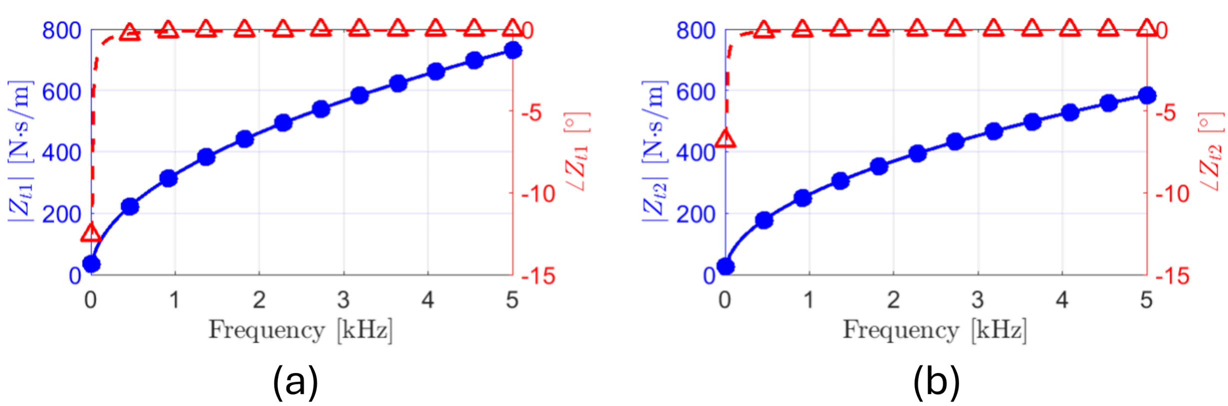


**Fig. 5** Magnitude (blue) and phase (red) of the exact and approximated torsional impedances ($Z_{t1}$, $Z_{t2}$). Exact impedances for the (a) left and (b) right-hand sides of the beam are in solid blue and dashed red lines, while the approximated values are dotted for the magnitude and triangles for the phase

which is close to the scale of precision for double float variables and suggests that this method is capable of extracting the boundary impedances exactly within the parameters of the assumed information.

## Conclusion

Decades of research in the area of steady-state traveling wave generation have stated that the necessary excitation conditions to produce a pure progressive wave have been sensitive to the boundary conditions of the structure. This work has shown that this sensitivity can be leveraged in the reverse direction: the excitation conditions can be used to approximate the impedance of the boundary conditions for a simple 1D Euler-Bernoulli beam. This has been done analytically, presuming that the user has complete knowledge of the structure's impedance and material properties.

Further work is necessary to fully implement this method experimentally. Namely, it is difficult to identify the loading ratios for exact excitation of traveling waves. Although there are many metrics to evaluate the quality of traveling waves, these most often consider the ratio of the left and right traveling waves ignoring the presence of the evanscent waves. Algorithmically identifying the loading ratios for these pure traveling waves is the next challenge that must be considered.

## References


1. D. J. Ewins, *Modal testing: theory, practice, and application*, 2nd ed. Baldock, Hertfordshire, England ; Philadelphia, PA: Research Studies Press, 2000.
2. Z. Wen, D. Wu, and K. Nakamura, "A Miniature Traveling Wave Ultrasonic Linear Motor Utilizing Bimorph Transducers," *IEEE Transactions on Ultrasonics, Ferroelectrics, and Frequency Control*, vol. 71, no. 6, pp. 698–706, Jun. 2024. [Online]. Available: https://ieeexplore.ieee.org/document/10510491/
3. H. Hariri, Y. Bernard, and A. Razek, "Dual piezoelectric beam robot: The effect of piezoelectric patches' positions," *Journal of Intelligent Material Systems and Structures*, vol. 26, no. 18, pp. 2577–2590, Dec. 2015. [Online]. Available: https://journals.sagepub.com/doi/10.1177/1045389X15572013
4. V. Ruiz-Díez, J. Hernando-García, J. Toledo, A. Ababneh, H. Seidel, and J. L. Sánchez-Rojas, "Piezoelectric MEMS Linear Motor for Nanopositioning Applications," *Actuators*, vol. 10, no. 2, p. 36, Feb. 2021. [Online]. Available: https://www.mdpi.com/2076-0825/10/2/36
5. D. Fleishman, Y. Asscher, and M. Urbakh, "Directed transport induced by asymmetric surface vibrations: making use of friction," *Journal of Physics: Condensed Matter*, vol. 19, no. 9, p. 096004, Mar. 2007. [Online]. Available: https://iopscience.iop.org/article/10.1088/0953-8984/19/9/096004
6. S. Daniel, M. K. Chaudhury, and P.-G. de Gennes, "Vibration-Actuated Drop Motion on Surfaces for Batch Microfluidic Processes," *Langmuir*, vol. 21, no. 9, pp. 4240–4248, Apr. 2005. [Online]. Available: https://pubs.acs.org/doi/10.1021/la046886s
7. A. Omidi Soroor and P. A. Tarazaga, "Non-reflective traveling waves in finite thin beams: A parametric study," *Thin-Walled Structures*, vol. 208, p. 112839, Mar. 2025. [Online]. Available: https://linkinghub.elsevier.com/retrieve/pii/S0263823124012783
8. V. V. N. S. Malladi, D. Avirovik, S. Priya, and P. Tarazaga, "Characterization and representation of mechanical waves generated in piezo-electric augmented beams," *Smart Materials and Structures*, vol. 24, no. 10, p. 105026, Oct. 2015. [Online]. Available: https://iopscience.iop.org/article/10.1088/0964-1726/24/10/105026
9. R. Gabai and I. Bucher, "Excitation and sensing of multiple vibrating traveling waves in one-dimensional structures," *Journal of Sound and Vibration*, vol. 319, no. 1-2, pp. 406–425, Jan. 2009. [Online]. Available: https://linkinghub.elsevier.com/retrieve/pii/S0022460X08005609
10. R. Gabay and I. Bucher, "On Vibrating Traveling Waves Actuation, Sensing, and Tuning in Finite Structures," in *Design Engineering and Computers and Information in Engineering, Parts A and B*. Chicago, Illinois, USA: ASMEDC, Jan. 2006, pp. 809–817. [Online]. Available: https://asmedigitalcollection.asme.org/IMECE/proceedings/IMECE2006/47675/809/322339
11. N. Tanaka and Y. Kikushima, "Active Wave Control of a Flexible Beam : Proposition of the Active Sink Method," *JSME international journal. Ser. 3, Vibration, control engineering, engineering for industry*, vol. 34, no. 2, pp. 159–167, 1991.
12. M. Kuribayashi, S. Ueha, and E. Mori, "Excitation conditions of flexural traveling waves for a reversible ultrasonic linear motor," *The Journal of the Acoustical Society of America*, vol. 77, no. 4, pp. 1431–1435, Apr. 1985. [Online]. Available: https://pubs.aip.org/jasa/article/77/4/1431/785595/Excitation-conditions-of-flexural-traveling-waves
13. Y. Tomikawa, K. Adachi, H. Hirata, T. Suzuki, and T. Takano, "Excitation of a Progressive Wave in a Flexurally Vibrating Transmission Medium," *Japanese Journal of Applied Physics*, vol. 29, no. S1, p. 179, Jan. 1990. [Online]. Available: https://iopscience.iop.org/article/10.7567/JJAPS.29S1.179
14. P. M. Daborn, "Smarter Dynamic Testing of Critical Structures," Ph.D. dissertation.
15. S. S. Rao, *Vibration of continuous systems*. Hoboken, N.J: Wiley, 2007, oCLC: ocm65301593.